THE JOHNS HOPKINS UNIVERSITY
CHARLES & 34th STREETS, BALTIMORE, MARYLAND 21218

NAG5-32

Geoid Anomalies and Fracture Zones in the Pacific Ocean

The SEASAT geoid anomalies of high degree and order ($n,m \geq 13$) in the central Pacific have been found to correlate closely with relative plate age. Steps in seafloor topography across fracture zones mark relative age offsets which produce a similar step in the geoid. An age offset of 10 m.y., in relatively young seafloor, across a fracture zone will result in a geoid anomaly of about 2 meters, and since such large age differences aee seen along major fracture zones,it is to be expected that these fractures will determine the geometry of the geoid anomalies. The east-west trending anomalies of alternating sign are framed by the regions of plate bounded by major fracture zones at nearly regular spatial intervals of about 1000 km. (Fig. 1)

The high degree and order geoid field in the Pacific is a superposition of fracture zone anomalies and hot-spot swell anomalies. A two-dimensional spectral analysis of this field reveals a very strong north- south wavenumber contribution with a dominant wavelength of about 2000 km, a much smaller contribution from east-west wavenumbers, and negligible contributions from other directions. (Fig. 2). To appreciate the magnitudes of the north-south and east-west components, we have taken one-dimensional profiles. (Fig. 3). A calculated geoid anomaly using an idealized fracture zone model (fig. 4) contains just about the same

(E84-10052) GEOID ANOMALIES AND FRACTURE ZONES IN THE PACIFIC OCEAN (Johns Hopkins Univ.) 11 p HC A02/MF A01 CSCL 08B
N84-14572
Unclas
G3/43 00052

amount of power in the 2350 km band wavelength as does the north-south profile of the SEASAT geoid field. In attempting to correlate plate age with geoid anomalies, a digitized age map of the Pacific has been used to generate a synthetic geoid, which has been subtracted from SEASAT. (Figs. 5-3). This procedure produces a residual geoid in which the fracture zone anomalies appear to be diminished, if not removed.

Acknowledgements

This work was supported by N.A.S.A. grant NAG5-32 to The Johns Hopkins University.

FIGURE CAPTIONS

Figure 1: Region in the central Pacific used in this study. Note the location of fracture zones relative to the geoid anomalies.
Latitude: -23° to 40°
Longitude: 180° to 243°

Figure 2: High-pass filtered power spectrum of central Pacific SEASAT geoid. Contour interval is 50 units.

Figure 3(a): Plot of N-S axis of power spectrum in figure 2.
(b): Plot of E-W axis of power spectrum in figure 2.

Figure 4(a): Series of idealized fracture zones with spacing of 1100 km.
(b): N-S profile of geoid height obtained using fracture zone model in (a).
(c): Log plots of power spectra of fracture zone model geoid and N-S SEASAT geoid.

Figure 5: Synthetic geoid obtained using absolute ages of seafloor. Contour interval is 1 m.

Figure 6(a): Full SEASAT geoid. Contour interval is 10 m.
(b): Synthetic geoid in figure 5.
(c): Residual geoid obtained by subtracting geoid in (b) from geoid in (a).

Figure 7: Synthetic geoid obtained using relative ages of seafloor. Contour interval is 0.5 m.

Figure 8(a): High degree and order SEASAT geoid. Contour interval is 3 m.
(b): Synthetic geoid in figure 7.
(c): Residual geoid obtained by subtracting geoid in (b) from geoid in (a).

SEASAT MEAN SEA SURFACE MINUS GEM 10B (12,12) GEOID

2m CONTOUR
REF. NO. 81004

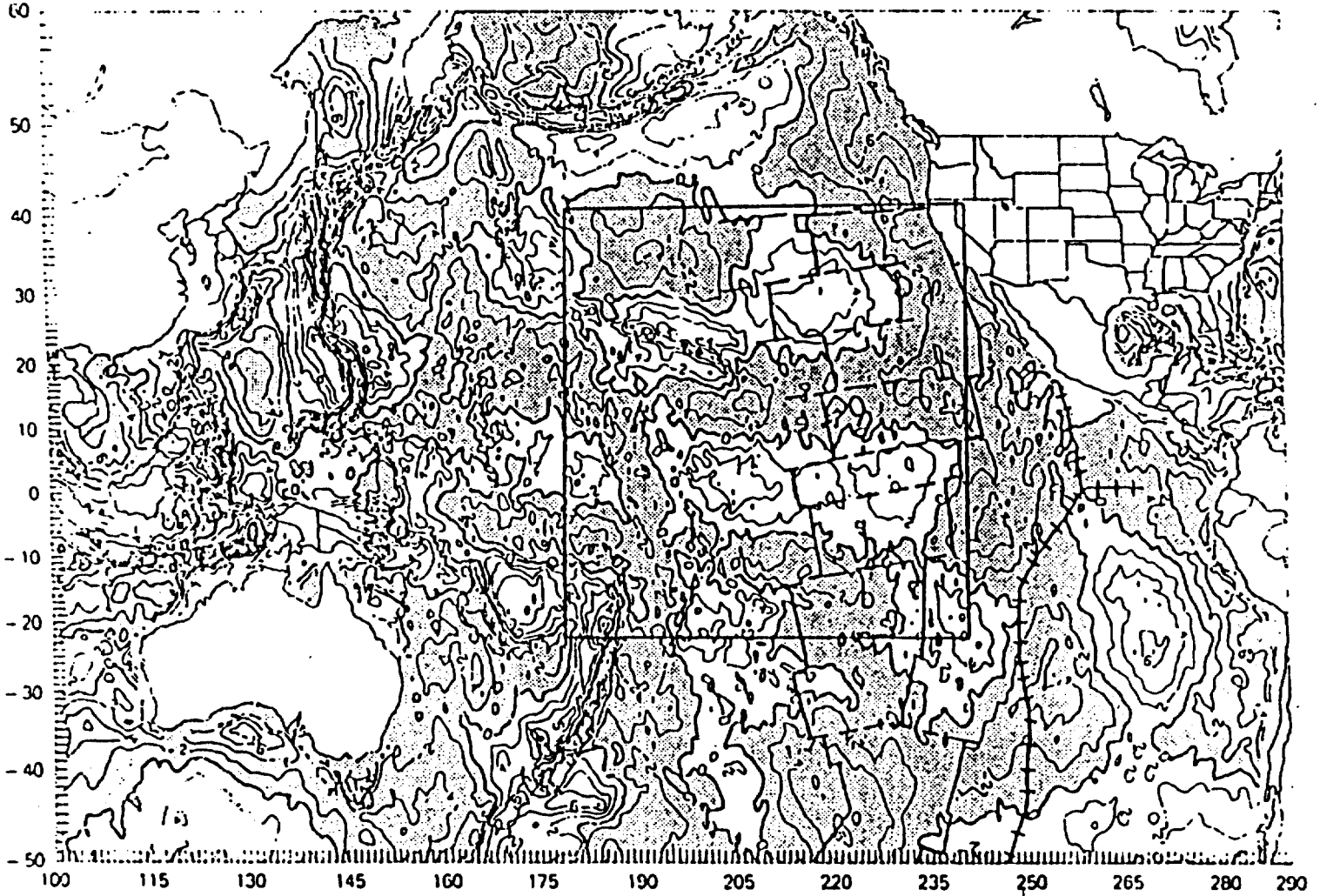

Figure 1.

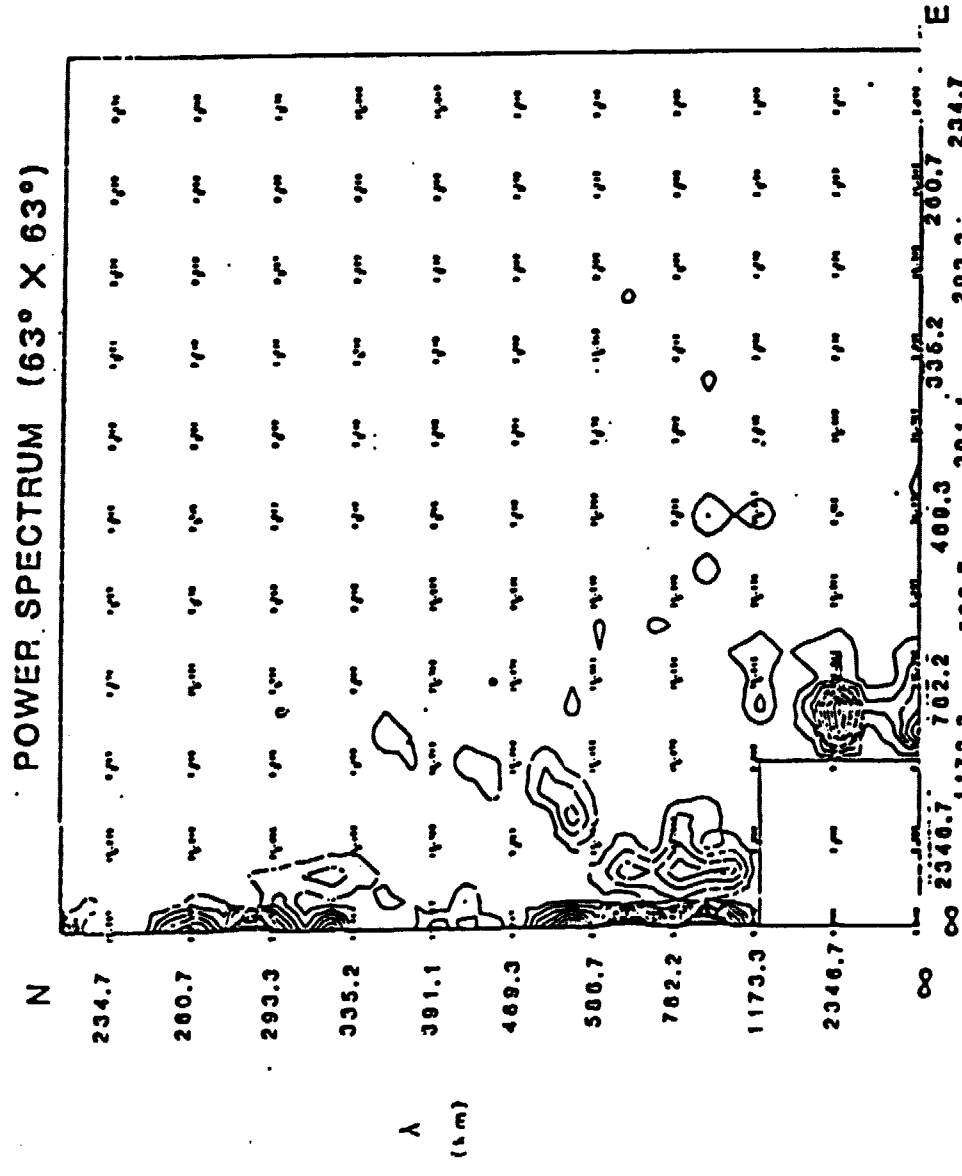

Figure 2

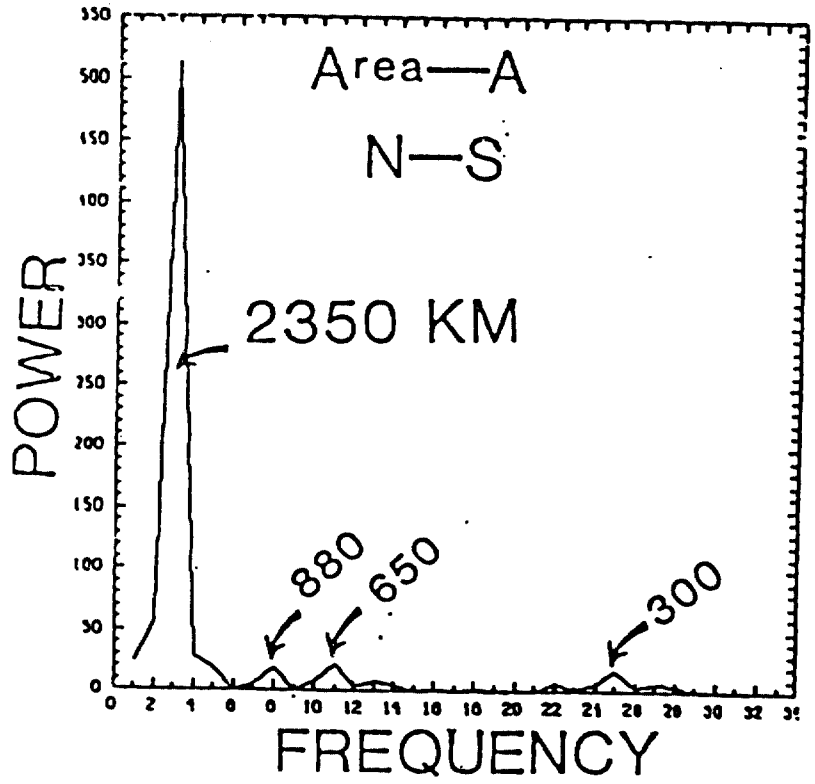

(a)

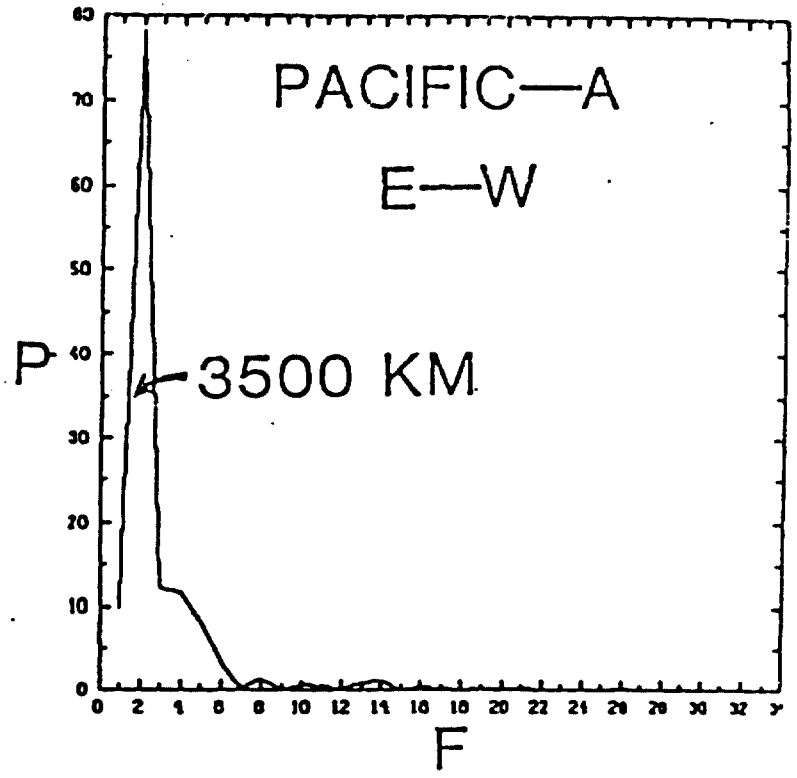

(b)

Figure 3

Idealized Fracture Zones

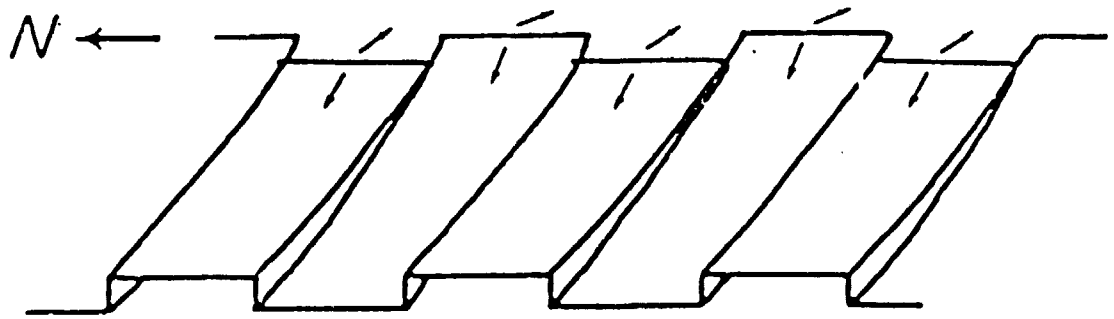

(a)

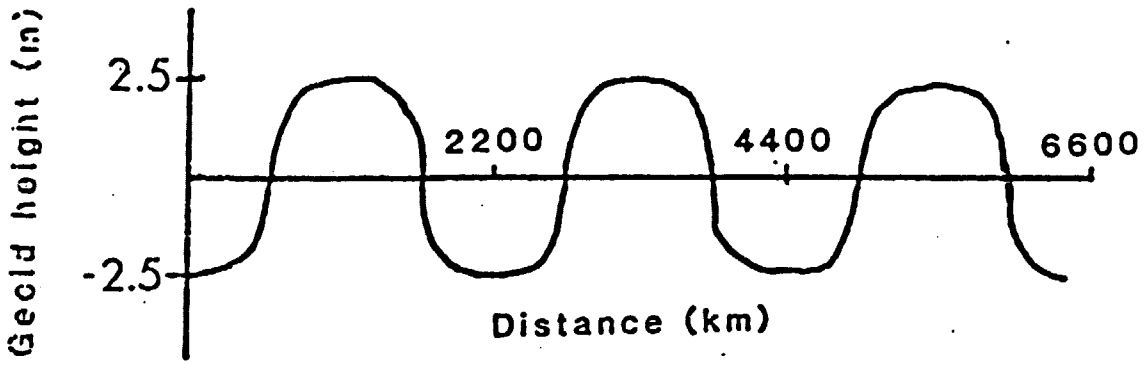

(b)

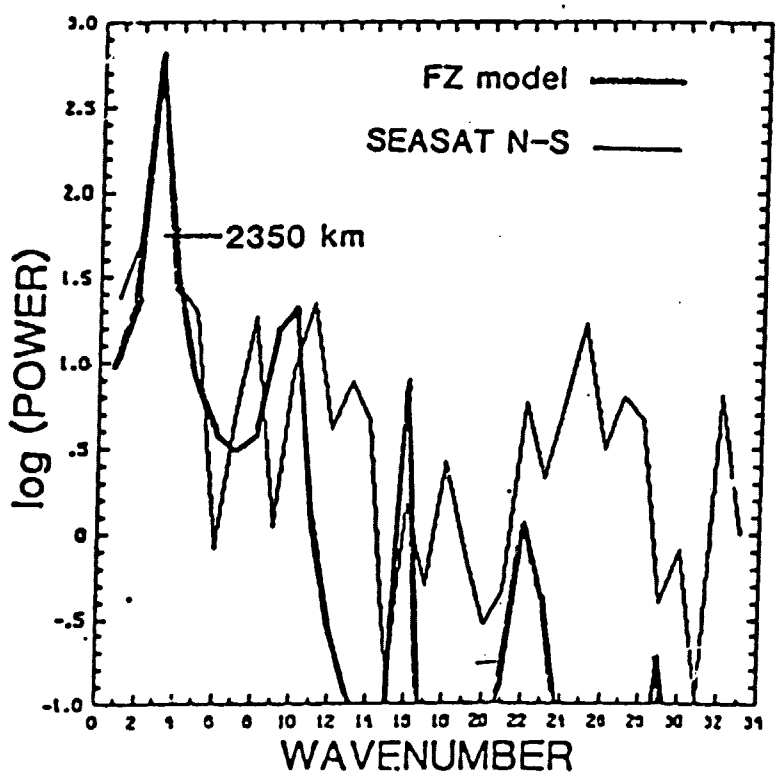

(c)

Figure 4

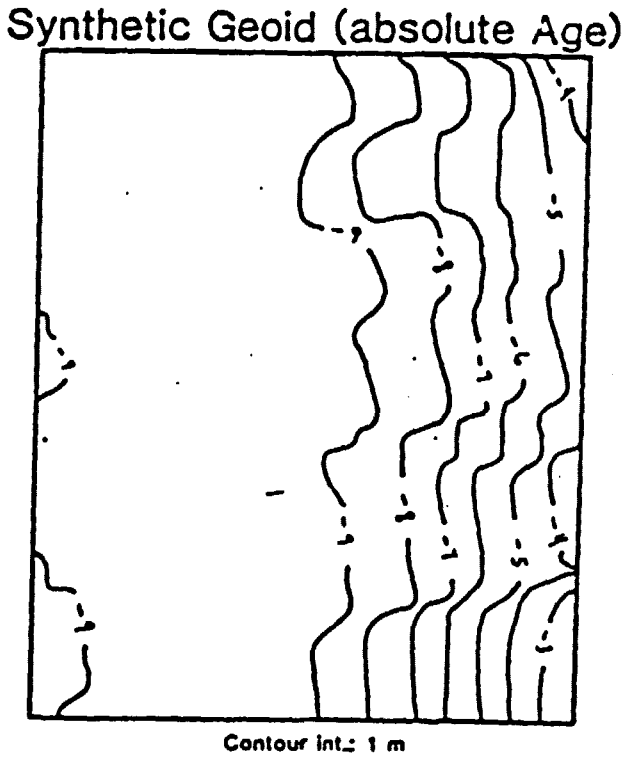

Figure 5

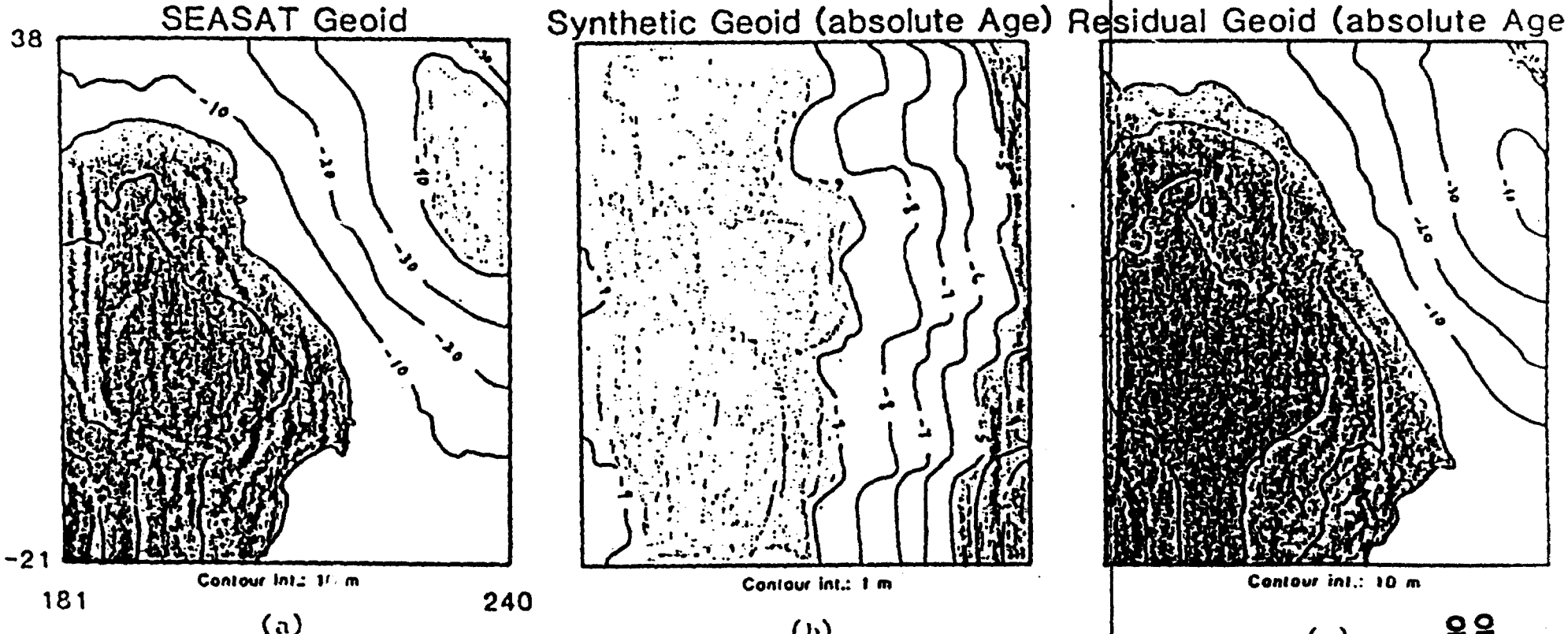

Figure 6

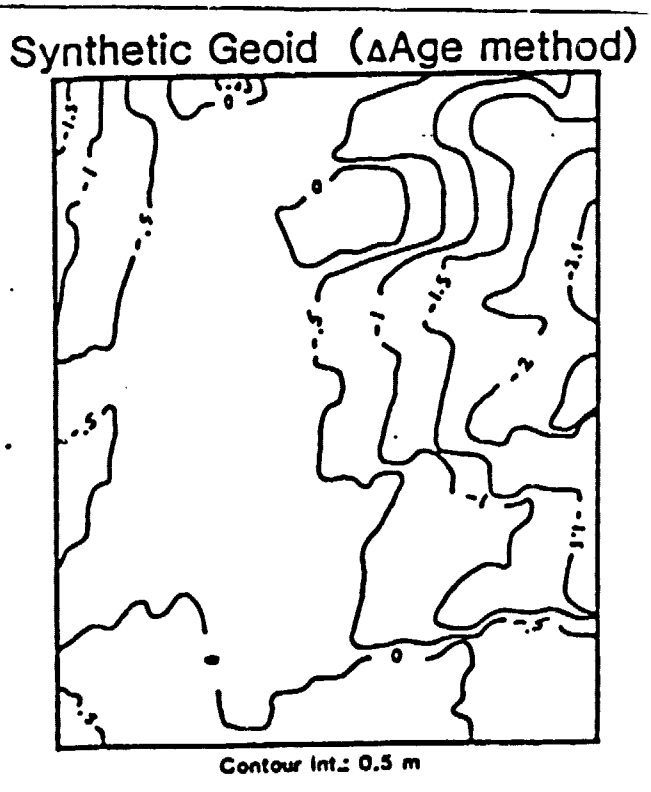

Figure 7

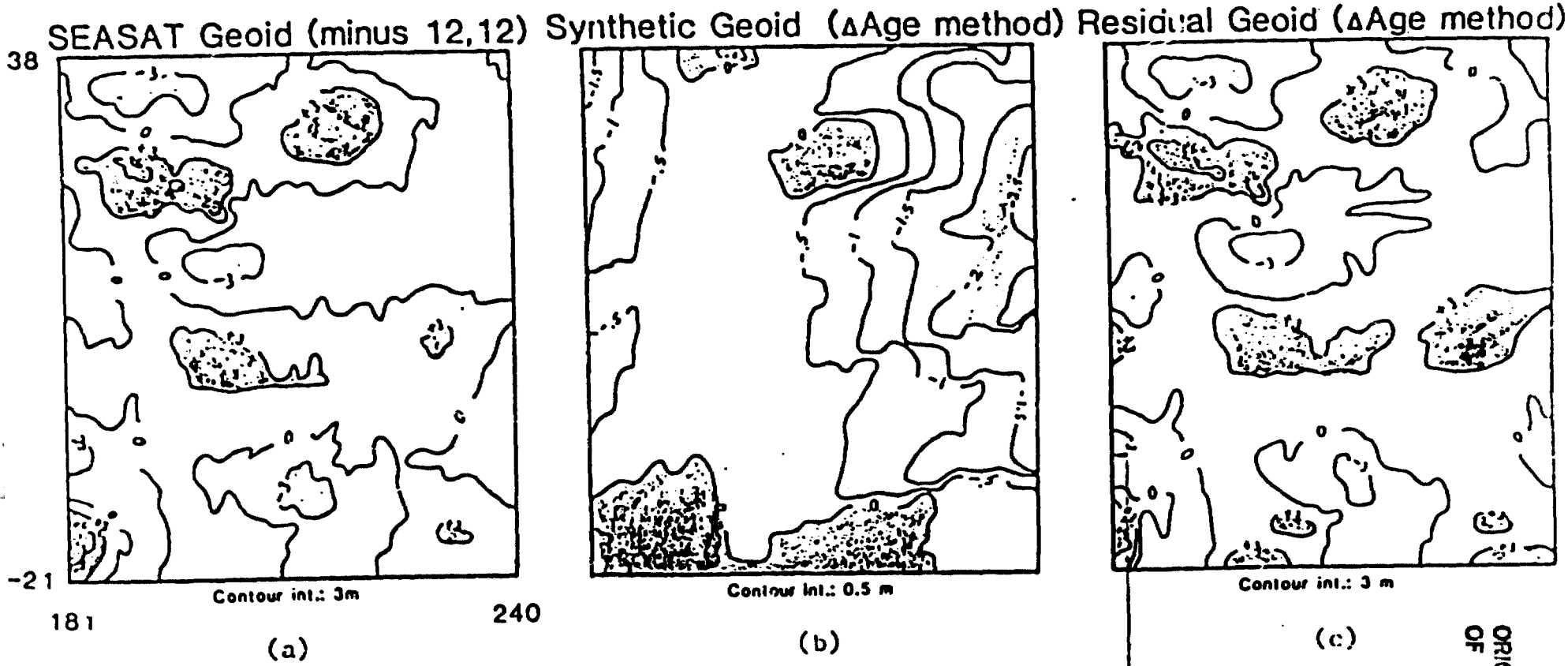

Figure 8